*geologica**acta*

Stable isotope geochemistry of the Ulldemolins Pb-Zn-Cu deposit (SW Catalonian Coastal Ranges, Spain)

P. ALFONSO [1] **C. CANET** [2] **J.C. MELGAREJO** [3] **J.M. MATA-PERELLÓ** [1] **A.E. FALLICK** [4]

[1] **Departament d'Enginyeria Minera i Recursos Naturals, Universitat Politècnica de Catalunya (UPC)**
Av. de les Bases de Manresa 61-73, 08242 Manresa, Barcelona, Spain. Alfonso E-mail: pura@emrn.upc.edu

[2] **Departamento de Recursos Naturales, Instituto de Geofísica, Universidad Nacional Autónoma de México**
Ciudad Universitaria, Del. Coyoacán, México DF, 04510, Mexico

[3] **Departament de Cristal·lografia, Mineralogia i Dipòsits Minerals, Facultat de Geologia, Universitat de Barcelona (UB)**
c/ Martí i Franquès, s/n, Spain

[4] **Isotope Geosciences Unit, Scottish Universities Environmental Research Centre**
East Kilbride, Glasgow, G75 0QF, Scotland (UK)

┤ A B S T R A C T ├

The Pb-Zn-Cu deposit of Ulldemolins occurs within the Carboniferous sedimentary series of the southernmost Catalonian Coastal Ranges. It consists of sulphide-bearing calc-silicate assemblages, with epidote, Ca-amphiboles and Ca-garnet, which develop selectively along a dolomicrite bed near the contact with a granite porphyry. Two mineralisation styles can be differentiated: a) banded and b) irregular. Fluid inclusions and stable isotope compositions of sulphur in sulphides (sphalerite, galena and chalcopyrite) and carbon and oxygen in carbonates (calcite and dolomite) were studied in order to constrain the genesis and the source of mineralizing fluids. Fluid inclusions in sphalerite and calcite are aqueous, liquid+vapour and have a salinity between 1.2 and 7.2 wt% NaCl eq. and homogenization temperatures in the range of 273° to 368°C. The $^{34}S_{(V-CDT)}$ values in the banded mineralisation are mostly between –1.5 and +2.1‰, and those from the irregular mineralisation are between –1.1 and +20.5‰. These ^{34}S values of the banded mineralisation are in agreement with a magmatic origin of sulphur. In addition, the $^{18}O_{(SMOW)}$ values of hydrothermal calcite, from +6.9 to +12.5‰, are consistent with a magmatic origin of the fluids that formed the banded ore deposit. Later, a new input of fluids interacted with the previously formed mineral assemblages and modified part of the deposit, leading locally to an irregular skarn mineralisation.

KEYWORDS | Ore deposits. Skarn. Calcsilicates. Stable isotopes. Fluid inclusions.

INTRODUCTION

The southern Catalonian Coastal Ranges include several ancient mining areas, most of them consisting of Pb-Zn vein deposits hosted by Paleozoic rocks. These deposits have produced more than 1Mt of ores since Roman times. Moreover, the Silurian and Carboniferous sedimentary series contain several tens of stratiform and banded base metal occurrences, which were ascribed to the sedimentary-exhalative type (SEDEX; Melgarejo, 1992; Canet, 2001; Alfonso *et al.*, 2002; Canet *et al.*, 2005).

The studied deposit is located about 3Km to the NE of the village of Ulldemolins, at 41°20'12''N-0°54'15''E, in the vicinity of the *Mas del Bessó* farm (Fig. 1, 2). The

supergene ores (secondary Cu carbonates) were mined during the Eneolithic (Vilaseca, 1973). These mines were also operative during short periods in the Middle Ages. Later, in the XIX century, these mines were known as the *Minas San Antonio*, but the fine grain size and complex character of the ores prevented their metallurgical processing, and thus giving up mining works. However, the banded morphology of the deposit induced the *Real Compañía Asturiana de Minas* to explore it during the 1960s, establishing about 250,000 tons of an average grade of 2.5wt% Pb, 2.5wt% Zn, 0.5wt% Cu, 80ppm Ag and 500ppm Cd, after a drilling survey of the reserves.

For a long time, the deposit has been considered as an example of the SEDEX type, owing to its apparent stratiform morphology (Melgarejo, 1992). Otherwise, considering the extensive development of calc-silicates in this deposit, Canet (2001) suggested that the deposit could be an example of "inhalites" produced by replacement of limestone bodies. This study presents data on the geology, fluid inclusions and stable isotopes of the Ulldemolins deposit. The principal goals of the study are to determine the origin of the ore-forming fluids, and to elucidate the genesis of the deposit.
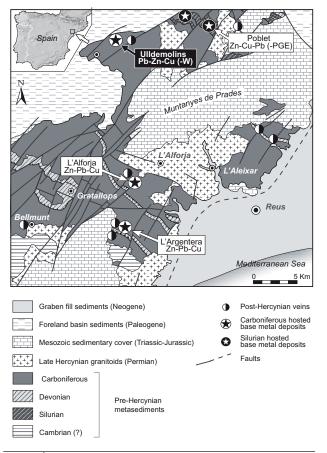

FIGURE 1 | Geological map of the southern Catalonian Coastal Ranges, with the location of the main base metal sulphide occurrences.

GEOLOGICAL SETTING

The Catalonian Coastal Ranges consist of a Hercynian folded basement unconformably covered by Mesozoic sedimentary rocks (Fig. 1). The basement is formed by early Cambrian to Devonian sedimentary rocks unconformably followed by a turbiditic Carboniferous Culm sequence (Melgarejo, 1992; Sanz-López *et al.*, 2000).

At the base of the Carboniferous sequences a cherty unit (up to 10m thick) occurs; it has been attributed to the Tournaisian. The Culm facies, up to 2000m-thick (Anadón *et al.*, 1985), contains several sedimentary exhalative Pb-Zn-Cu-Ag occurrences (Melgarejo, 1992; Canet, 2001). It starts with the coarse-grained Bassetes Unit, ~400m thick, which is composed of greywackes and conglomerates, with interstratified olistoliths of chert and limestones. On the basis of its conodont fauna, this informal unit, which contains the massive sulphide ore body of L'Argentera (Alfonso *et al.*, 2002), has a Visean age (Anadón *et al.*, 1985). The following Ulldemolins Unit has a similar thickness and is essentially pelitic, with minor interbedded sandstones (Sáez, 1982). It also contains limestone olistoliths and minor trachytes (Melgarejo, 1992). This unit contains the Pb-Zn-Cu sulphide deposits of Ulldemolins and L'Alforja, and is Visean to Lower Namurian in age (Sáez, 1982).

The Hercynian orogenesis affected the Paleozoic series throughout the development of two episodes of folding and thrusting accompanied by very low-grade regional metamorphism. The first deformation produced NNW-SSE trending folds and thrusts with vergence to the WSW, whereas the second one produced folds and thrusts with vergence to the ENE.

Post-tectonic, Late Hercynian calc-alkaline granitic stocks, ranging from quartzdiorite to leucogranite, intruded the Hercynian sequences (Melgarejo and Ayora, 1984). Granite to tonalite porphyries crosscut all the above-mentioned Paleozoic series and granitic rocks. The intrusive rocks are Permian in age, according to Rb-Sr dating (Enrique and Debon, 1987), and produced contact metamorphism from pyroxene to amphibole hornfels facies. Some Late Hercynian NNW-SSE and NE-SW wrench faults have been reactivated as normal faults during the Alpine orogenesis, acting as conduits for hydrothermal fluids and producing Ba-Pb-Zn-Cu-Ni-Co-Ag veins (Canals and Cardellach, 1997).

METHODS AND CONDITIONS OF ANALYSIS

The extensive outcrops of the deposit and a complex system of trenches and galleries favoured a detailed

sampling. The samples have been studied in polished thin sections using a standard petrographic microscope. Scanning electron microscope (SEM) images and qualitative analyses were produced using a Cambridge Stereoscan 120 equipment, at the Serveis Cientificotècnics de la Universitat de Barcelona. The samples were examined in the backscattered electron mode (BSE). The mineral chemistry of silicates (epidote, chlorite, Ca-amphibole, Ca-garnet and feldspars), sulphides (sphalerite), and carbonates (calcite and dolomite), was quantitatively obtained with a CAMECA SX-50 electron microprobe at the *Serveis Cientificotècnics* of the Universitat de Barcelona.

Microthermometric measurements were performed on a Linkam THMS-600 stage. Calibration was made with standard compounds between -56.6ºC and 308.9ºC. The precision was ±0.2ºC for the freezing measurements and ±1ºC for the heating measurements. These ice melting temperatures were used to determine salinity data using the equations of Bodnar (1993).

Sulphur isotopes were measured in 20 samples of sphalerite, 12 of chalcopyrite and 11 of galena. Isotope analyses were carried out at the Scottish Universities Environmental Research Centre, in Scotland, UK. Samples were analyzed both as powder and directly on thick polished sections. In the first case, mineral separations were made by handpicking. Purity of the samples was tested by examination with a binocular microscope and by X-ray diffraction. *In situ* laser combustions were carried out with a Nd-YAG laser system following the method of Fallick *et al.*

(1992) and Hall *et al.* (1994); powder combustions were performed similarly and purified SO_2 was analyzed on a VG-SIRA II mass spectrometer. The results are given as $\delta^{34}S$‰ values relative to the Vienna-Canyon Diablo Troilite (V-CDT) standard. The lateral resolution of the laser beam is about 250µm; the analytical precision is within ±0.2‰ at 1. Additional samples were analysed by mass spectrometry using a Delta C Finnigan MAT continuous flow isotope-ratio mass spectrometer with an elemental analyzer, a TC-EA according to the method of Giesemann *et al.* (1994). These analyses were carried out at the *Serveis Cientificotècnics* of the Universitat de Barcelona.

Six representative samples of hydrothermal carbonates were selected for carbon and oxygen isotope analyses. Three samples of carbonates are comprised of dolomite from the dolostone of the banded mineralisation and another three are made up of calcite from the irregular mineralisation. Oxygen and carbon stable isotope measurements were carried out at the *Serveis Cientificotècnics* of the Universitat de Barcelona, with a Finnigan Delta-S mass spectrometer. The extraction of CO_2 from carbonates for isotope analysis followed standard techniques of McCrea (1950). The oxygen values are reported in δ‰ relative to V-SMOW, whereas carbon values are reported in δ‰ relative to Vienna-Pee Dee Belemnite (V-PDB) standard. The $\delta^{18}O$ compositions of water in equilibrium with carbonate minerals were calculated using temperatures from 300º to 500ºC, estimates based on mineralogy and fluid inclusion data. Water compositions were calculated using the equation of O'Neil *et al.* (1969).
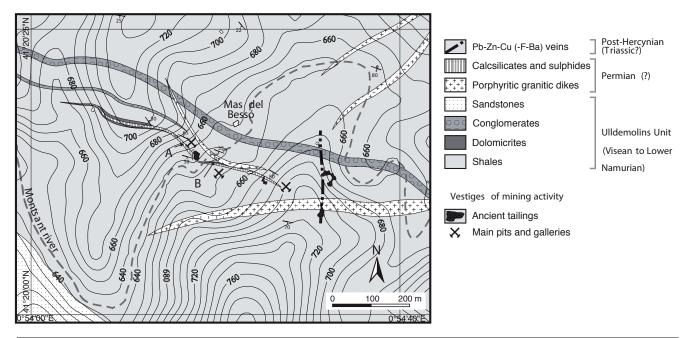

FIGURE 2 | Detailed geological map of the area of the Ulldemolins deposit and the Mas del Bessó farm.

STRUCTURE OF THE DEPOSIT

The Ulldemolins deposit is hosted by Lower Namurian turbiditic sequences that, in the vicinity of the deposit, consists of a 150-200m thick coarse-grained unit of interbedded sandstones, pelites and conglomerates, followed by ~200m of grey shales (Fig. 3). At the top of the coarse-grained unit, a dolomicrite bed, up to 5m thick, hosts the ore mineralisation.

The ore-bearing dolomicrites are exposed along 500m, and crop out in the inverted limb of a recumbent Hercynian NE-trending fold. The dolomicrite beds strike approximately EW, with a dip of 50-65°N, and attain a maximum thickness of about 5m. Several late Hercynian porphyritic granitic dykes intruded the series and structures described above. Subconcordantly with the sedimentary series, a ~6m thick, WNW-ESE trending, porphyritic granitic dyke is partly in contact with the ore bearing dolomicrites. A magmatic breccia-dyke, up to 1m wide, occurs close to the contact between the dyke and the mineralized dolomicrites. Centimeter-sized fragments of this breccia, consisting in shales and ore, are embedded in an aphanitic matrix (Fig. 3).

According to the morphology of the ores and their position with respect to the granite porphyry, two types of mineralisation can be distinguished: a) banded and b) irregular.

Banded mineralisation

The banded mineralisation consists of lens-shaped bodies, rich in sulphides and calc-silicates, extending more than
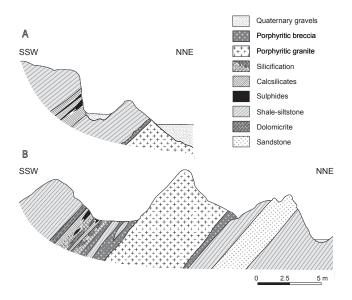

FIGURE 3 | Geological cross-sections of the ore mineralisation of the Ulldemolins deposit, showing the two mineralisation types that are recognisable at outcrop scale: A) banded, and B) irregular.

1500m long with a thickness ranging from several cm to 3m. The lenses are interbedded in the dolomicrite bed. They exhibit a rough banding, defined by alternating sulphide- and calc-silicate-rich layers from some centimetres to several tens of centimetres wide. In addition, minor feldspar-rich and shale layers are found. Sulphide-rich layers are mainly composed of sphalerite, chalcopyrite, galena, marcasite and minor magnetite, whereas the calc-silicate-rich ones are rich in epidote, Ca-amphibole, chlorite, quartz and calcite.

Epidote is the most abundant silicate in the Ulldemolins deposit. It forms decimetre-thick, roughly stratiform bodies that, macroscopically, show a weakly layered structure. In addition, irregular epidote veinlets, a few millimetres wide, crosscut the layering (Fig. 4). Chlorite and quartz occur interstitially with respect to epidote.

Feldspar-rich layers occasionally occur near the contact between the host grey shales and the calc-silicate-rich layers, and are composed by nearly pure K-feldspar or by Ca-plagioclase, with minor amounts of epidote, quartz, muscovite, monazite, rutile and titanite.

Sulphide-rich layers, up to 50cm wide, are massive or roughly banded, with interbedded ferroactinolite. They consist mainly of sphalerite and chalcopyrite with minor galena, pyrite and marcasite; sulphides also occur in minor veinlets that crosscut the banded mineralisation (Fig. 4).

Irregular mineralisation

This mineralisation occurs as irregular bodies near the contact between carbonated rocks and the granite porphyry. It consists mainly of scheelite with a powellite-rich core, galena and sphalerite, with minor pyrite, marcasite, chalcopyrite, hematite and titanite disseminated within the dolomicrite bed, which is mostly silicified. Other minerals present are Ca-amphibole, Ca-garnet, diopside and chlorite. Replacement textures are abundant (Fig. 5).

PARAGENESIS AND MINERAL CHEMISTRY

Some representative textures of the mineralisation are provided in Figure 5, and the sequence of crystallisation of the mineralisation is shown in Figure 6.

Silicates

Epidote is the most abundant silicate in the deposit, although it only occurs in the banded mineralisation. Three textural types of epidote can be distinguished: a) fine-grained, up to 25μm in length, subhedral epidote occurring in monomineralic, layered beds;

b) coarse-grained, up to 150μm in length, euhedral epidote crystals or aggregates embedded into a sulphide groundmass, and c) epidote veinlets. The three textural types do not show significant differences in chemical composition. In all cases, the clinozoisite end-member ($Ep_{40-11}Czo_{90-60}Pie_{3-0}$) is dominant and the Mn content is low, up to 1.27wt% Mn_2O_3 (Fig. 7A, Table 1). Epidote crystals exhibit a concentric zoning caused by changes in the concentration of Al and Fe^{3+}, the latter being in higher concentrations towards the rim of the crystals.

Ca-amphiboles are abundant in the banded mineralisation, whereas in the irregular mineralisation they occur only in minor amounts. Two textural types of Ca-amphiboles can be distinguished: a) fine-grained, up to 30μm in length, fibrous aggregates, which occur associated with minor epidote and disseminated sulphides, and b) coarse-grained prismatic crystals, up to 200μm in length, included in a sulphide groundmass (Fig. 5A). All of them belong to the tremolite-ferroactinolite series, ranging in composition from actinolite to ferroactinolite (Fig. 7C, Table 1).

Ca-garnet occurs in the irregular mineralisation, in the silicified dolomicrites where it constitutes roughly banded aggregates (Fig. 4A). Ca-garnet crystals are euhedral to subhedral, up to several millimetres in diameter, and often exhibit concentric zoning (Fig. 5C). They are grossular in composition (Gr_{70-95}). The MnO content varies from 1.2 to 5.7wt% in the irregular mineralisation and from 1.1 to 7.7wt% in the banded mineralisation (Fig. 7B, Table 1).

Chlorite occurs as fine-grained platy crystals, often developing radial aggregates. It occurs interstitially with respect to epidote grains, and forms pseudomorphs after Ca-garnet. They are trioctahedral chlorites of the clinochlore-chamosite series with an average of 2.92Mg atoms per formula unit (*apfu*), 1.49 Fe *apfu*, and 3.07 Si *apfu* (Table 1).

Quartz is abundant in the entire deposit and mostly occurs as anhedral crystals, up to several millimetres in size, showing granoblastic, sutured, poikiloblastic textures, very rich in solid inclusions of epidote, ferroactinolite and dolomite.

The irregular mineralisation contains feldspar-rich centimetre-thick bands, interbedded within the shale. These feldspars are bytownite in composition (An_{75-81}), with an orthoclase component below 3.2%. In the banded mineralisation, minor adularia (K-feldspar, Or_{94-100}) occurs as monomineralic, millimetre-thick bands. The albite component is up to 6%, and barium contents ranges from 0.6 to 1.85wt% BaO (Table 1).

Carbonates

Dolomite from the host dolomicrites has micritic texture, and the chemical composition of carbonates is broadly constant, corresponding to pure dolomite.

In the banded mineralisation, pure calcite occurs in veinlets and associated with the quartz that is rich in epidote inclusions.
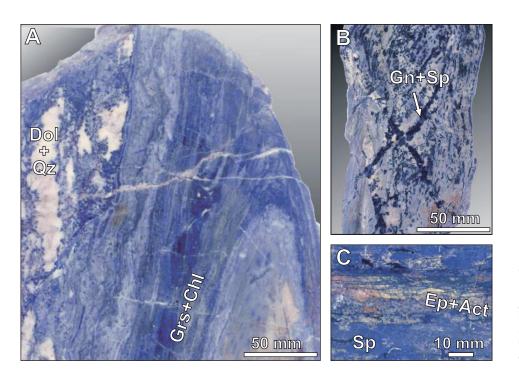

FIGURE 4 | Hand specimens of the Ulldemolins deposit, showing complex textures between sulphides, carbonates and calc-silicates. A) Irregular mineralisation with calcsilicate layered aggregates and sulphide and quartz-carbonate veinlets; B) sphalerite-rich, banded mineralisation. Act: actinolite; Chl: chlorite; Dol: dolomite; Ep: epidote; Gn: galena; Grs: grossular; Sp: sphalerite.

On the other hand, the irregular mineralisation carbonates show a more varied composition, with 50-65 molar% $CaCO_3$, 40-50 molar% $MgCO_3$, and 5-30 molar% $FeCO_3$.

Ore minerals

Sphalerite is the most abundant sulphide mineral in the banded mineralisation, followed by chalcopyrite, galena, magnetite, pyrite and marcasite. Galena is more abundant in the irregular mineralisation. Ore minerals occur disseminated interstitially within the calc-silicate-rich assemblages or forming massive, millimetre-sized aggregates (Fig. 4, 5). Galena, sphalerite and chalcopyrite

occur in the banded mineralisation as anhedral grains.

Sphalerite is rich in chalcopyrite blebs. The chemistry of sphalerite shows significant variations between the banded and the irregular parts of the mineralisation (Fig. 8). In the banded mineralisation, iron content varies between 5.5 and 11.1wt% Fe, whereas in the irregular mineralisation it exhibits a wider range of values, between 7.5 and 14.5wt% Fe. Likewise, manganese content is also higher in the sphalerite from the irregular mineralisation, with 0.5 to 1.3wt% Mn, whereas in the banded one it is less than 0.4wt% Mn. The concentration in cadmium is similar in both mineralisation types, from 0.4 to 1.1wt% Cd (Table 2).
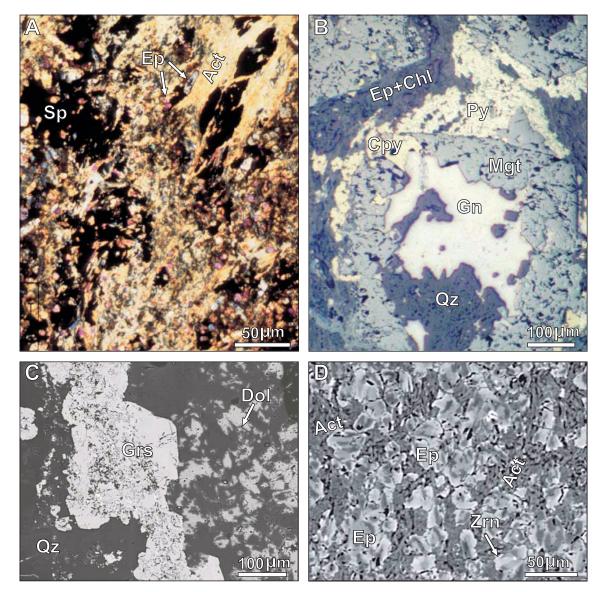

FIGURE 5 | Microscopic textures of mineral assemblages from the Ulldemolins deposit. A) Plane polarized light; B) reflected light; C, D) SEM-BSE images. Act: actinolite; Chl: chlorite; Cpy: chalcopyrite; Dol: dolomite; Ep: epidote; Gn: galena; Grs: grossular; Mgt: magnetite; Py: pyrite; Qz: quartz; Sp: sphalerite; Zrn: zircon.

FIGURE 6 | Episodes and sequence of crystallisation of mineral assemblages in the Ulldemolins deposit.

TABLE 1 | Chemical composition and structural formulas of selected silicates from the Ulldemolins deposit (electron-microprobe data)

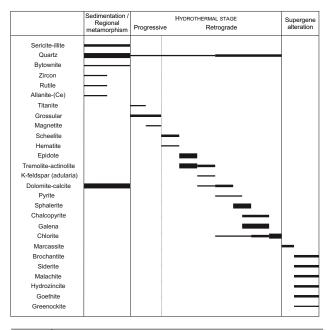|		Ep		Act		Chl	Grs		Kfs
		#1	#2	#3	#4	#5	#6	#7	#8
SiO_2	wt. %	37.26	37.77	52.33	53.87	34.73	37.15	39.66	63.84
Al_2O_3		22.79	22.11	1.83	1.164	14.32	19.09	18.13	18.53
TiO_2		0.049	0.10	0.10	0.06	0.02	0.47	0.37	–
CaO		22.94	22.98	11.50	12.56	0.31	31.18	34.10	0.00
Na_2O		0.00	0.00	0.12	0.08	0.05	0.03	0.00	0.31
K_2O		0.00	0.01	0.08	0.07	0.03	–	–	15.24
BaO		–	–	–	–	–	–	–	1.33
MnO		0.42	0.42	1.21	1.07	0.10	5.66	0.75	–
Fe_2O_3		14.49	14.74	–	–	–	3.69	6.03	–
FeO		–	–	22.26	15.72	17.41	1.71	0.71	0.08
MgO		0.41	0.00	9.27	13.29	20.97	0.03	0.10	0.00
F		0.00	0.23	–	–	0.26	–	–	–
Cl		0.00	0.013	–	–	0.08	–	–	–
H_2O		1.88	1.76	1.86	2.05	11.94	–	–	–
Total		100.24	100.03	100.56	99.93	100.09	99.01	99.85	99.33
Si	Apfu	3.183	3.248	7.601	7.502	3.444	2.923	3.022	2.993
Al		2.295	2.241	0.129	0.240	1.670	1.767	1.625	1.024
Ti		0.003	0.007	0.000	0.010	0.001	0.028	0.021	–
Ca		2.100	2.117	1.855	1.880	0.033	2.624	2.852	0.000
Na		0.000	0.000	0.022	0.015	0.010	0.005	0.000	0.028
K		0.000	0.002	0.009	0.010	0.004	–	–	0.912
Ba		–	–	–	–	–	–	–	0.000
Mn^{2+}		0.030	0.031	0.272	0.182	0.008	0.376	0.048	–
Fe^{3+}		0.933	0.955	–	–	–	0.218	0.345	–
Fe^{2+}		–	–	1.833	2.408	1.442	0.112	0.045	0.003
Mg		0.053	0.000	2.711	2.238	3.095	0.004	0.012	0.000
F		0.000	0.110	–	–	0.083	–	–	–
Cl		0.000	0.003	–	–	0.013	–	–	–
OH^{-*}		1.000	0.887	2.000	2.000	8.000	–	–	–

Apfu; atoms per formula unit. Act, Ca amphiboles (structural formula based on 22 O and 2 OH), ferroactinolite. Chl, chlorites (structural formula based on 18 O, OH), clinochlore-chamosite. Grs, Ca garnets (structural formula based on 12 O), grossular. Ep, epidote (structural formula based on 12 O and 1 OH). Kfs: K feldspars (structural formula based on 8 O), adularia.
*Only the hydroxyl group (combined water).

FLUID INCLUSIONS

Fluid inclusions were investigated in sphalerite and calcite from the banded and the irregular mineralisations, respectively. Fluid inclusions occur homogeneously distributed or in planes; the last were discarded in this study, as being of secondary origin according to criteria provided by Roedder (1984). Hence, inclusions showing evidences of post-entrapment modifications, such as necking down, were also avoided for microthermometric measurements. Thus, only primary fluid inclusions were measured. Primary fluid inclusions, both in sphalerite and calcite, have a regular morphology and small size, usually between 2 and 5μm, and are aqueous two-phase liquid-vapour (L+V), with the bubble representing 5-15vo% of the inclusion at room temperature.

The microthermometric results are represented in Figure 9. Fluid inclusions in sphalerite from the banded mineralisation show a narrow range in homogenization temperatures (T_h) and salinities. T_h is between 270° and 310ºC, and the ice melting temperatures (T_{mi}) range from -2.1° to -0.8ºC, corresponding to a salinity of 1.4–3.5wt% NaCl equivalent. Fluid inclusions in calcite of the irregular mineralisation always homogenize to the liquid phase, with T_h ranging from 250° to 368ºC. T_{mi} ranges between -4.5 and -7.2ºC, which corresponds to a salinity of 1.2–7.2wt% NaCl equivalent.

The densities of the mineralizing fluids were calculated with the computer program "Fluids" of Bakker (2003), using the equation of Bodnar (1993). The obtained values are $0.75g/cm^3$ for the banded mineralisation, and from 0.70 to $1.02g/cm^3$ for the irregular mineralisation.

STABLE ISOTOPES

Sulphur isotopes

In the banded mineralisation, sulphides display a narrow variation of $\delta^{34}S$, from -1.5 to +2.1‰, except one value of +12.3‰ (Fig. 10, Table 3). Similar values occur in the magmatic breccia, with $\delta^{34}S$ values ranging from -1.1 to +0.8‰. Otherwise, sulphides from the replacive, irregular ore masses adjacent to the contact with the granite porphyry show a wider range of $\delta^{34}S$ values, from -1.1 to +20.6‰ (Fig. 10). The average $\delta^{34}S$ values in sulphide minerals of the entire deposit follow the sequence: sphalerite>chalcopyrite>galena. However, the temperatures obtained from the isotopic pairs, using the equations of Ohmoto and Rye (1979), usually are anomalously high and do not coincide between different mineral pairs. This indicates a lack of isotopic equilibrium during mineralisation, in agreement with the observed textural relationships of

the ores (*i.e.* replacement textures between sphalerite and chalcopyrite).

Carbon and oxygen isotopes in carbonates

The results of carbon and oxygen isotope analysis in carbonates are represented in Figure 11 and listed in Table
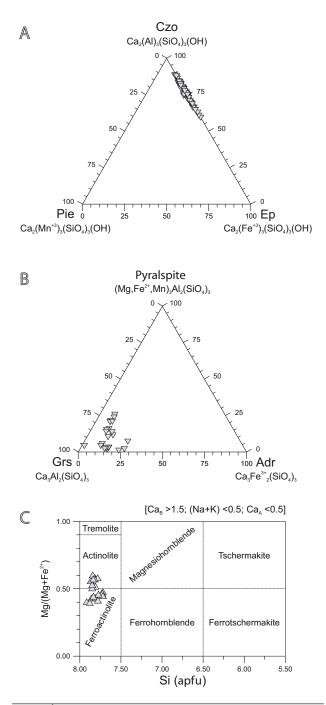
4. Dolomite from the banded mineralisation exhibits a narrow range in isotopic composition, with $\delta^{13}C$ from -2.6‰ to -0.1‰, and $\delta^{18}O$ from 8.5‰ to 9.3‰. On the other hand, calcite from the irregular mineralisation shows a different but still narrow range in the $\delta^{13}C$ values, from -9.2‰ to -7.7‰, but exhibits a larger variation in $\delta^{18}O$, from 6.9‰ to 12.5‰.

DISCUSSION

The Ulldemolins occurrences exhibit a calc-silicate-dominated mineral assemblage, with evidences of a complex, multi-event ore genesis, which is typical of skarns. Hydrous calc-silicates (epidote and Ca-amphibole) predominate over the anhydrous. Ca-garnet and Ca-pyroxenes are absent, as distinctive of retrograde skarns (Meinert, 1993). As in other skarns (*e.g.*, Einaudi, 1982), in the banded mineralisation, the stage of mineralisation has totally obliterated the prograde mineral association. In the irregular mineralisation, proximal mineralisation growth of Ca-garnet only occurs partially pseudomorphized by chlorite.

To elucidate the ore genesis processes responsible for the Ulldemolins Pb-Zn-Cu mineralisation, several facts must be considered:

1) Some textures, such as layering of calc-silicates and a rough mineral banding, could be interpreted as a sign that part of the mineralisation is syngenetic, taking place
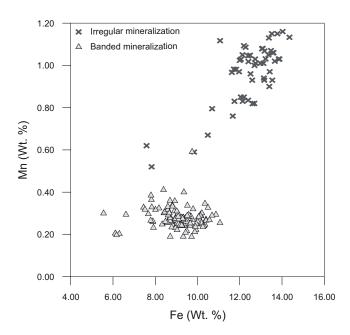
FIGURE 7 | Composition of different silicates from the Ulldemolins deposit. A) Minerals of the epidote group in clinozoisite (CZo) – piemontite (Pie) – Epidote (Ep) diagram. B) Calcic garnet in grossular pyralspite – (pyrope+almandine+spessartine) – andradite triangular plot. C) Classification of calcic amphiboles (Leake *et al.*, 1997).

FIGURE 8 | Fe *vs* Mn content of sphalerite from the Ulldemolins deposit.

		Banded			Irregular		
		#1	#2	#3	#4	#5	#6
S	wt.%	33.52	33.24	33.92	33.41	33.66	33.55
Zn		55.30	57.81	55.85	50.39	50.03	49.93
Fe		9.67	7.82	8.99	13.66	13.84	14.03
Cu		0.03	0.02	0.01	0.04	0.04	0.11
Cd		0.61	0.62	0.63	0.74	0.71	0.68
Mn		0.28	0.37	0.29	1.02	1.03	1.16
Ge		0.00	0.05	0.00	0.00	0.00	0.00
Total		99.41	99.93	99.69	99.26	99.31	99.46
S	atom %	50.369	49.977	50.752	50.018	50.262	50.058
Zn		40.759	42.634	40.994	37.003	36.643	36.541
Fe		8.343	6.750	7.724	11.741	11.865	12.019
Cu		0.023	0.015	0.008	0.030	0.030	0.083
Cd		0.261	0.266	0.269	0.316	0.302	0.289
Mn		0.246	0.325	0.253	0.891	0.898	1.010
Ge		0.000	0.033	0.000	0.000	0.000	0.000

before the intrusion of the dyke. However, these textures could reflect primary sedimentary layering of the protolith or can result from a reactive infiltration and hydrodynamics (Ciobanu and Cook, 2004), and have been observed in many skarns elsewhere (*e.g.*, Canet *et al.*, 2009).

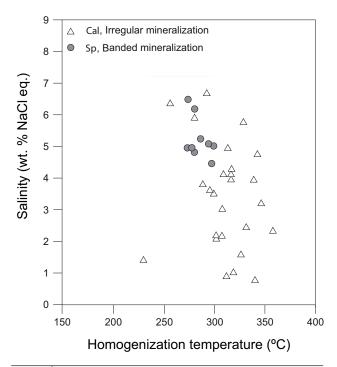2) The banded and irregular mineralisations show significant differences in all the geochemical data

presented here: mineral chemistry, stable isotopes and fluid inclusions. In general, these geochemical parameters are rather constant in the banded mineralisation, whereas the irregular mineralisation shows wider ranges of variation.

3) Sulphides from the banded mineralisation mainly exhibit a narrow range of $\delta^{34}S$, from -1.5 to +2.1‰. In contrast, in the irregular mineralisation, there are variations in $\delta^{34}S$, from -1.5 to +20.5‰. Several base metal sulphide occurrences have been reported in the Carboniferous series of the southern Catalonian Coastal Ranges (Canet *et al.*, 2005). They exhibit $\delta^{34}S$ values from -1.0 and +7.0‰ and an average of +4.4‰ (Canet *et al.*, 2005). The isotope composition of sulphides from the banded mineralisation would be consistent with a magmatic origin of sulphur (Ohmoto and Rye, 1979).

4) The only intrusive body that crops out in the area is a small granite porphyry. However, the possibility of the presence of a magmatic fluid is supported by the occurrence of magmatic breccia close to the sulphide occurrences. The possible existence of a blind, large intrusion beneath the deposit cannot be excluded. The presence of sulphide fragments with sharp borders, scattered into the barren magmatic matrix of the breccia, indicates that a sulphide mineralisation existed prior to its emplacement.
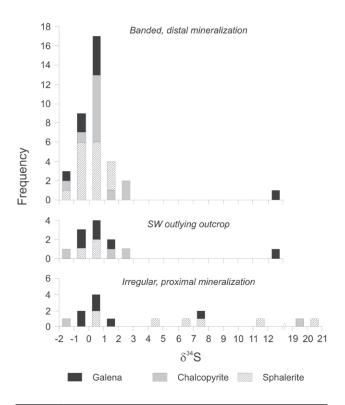

FIGURE 9 | Salinity versus homogenization temperature plot for fluid inclusions analysed from the Ulldemolins deposit. Cal: calcite; Sp: sphalerite.

FIGURE 10 | $\delta^{34}S$ values (CDT ‰) of sulphides of the Ulldemolins deposit.

TABLE 3 | Sulphur isotope data, δ³⁴S (‰ V-CDT), for sulphide minerals from the Ulldemolins deposit

Type of mineralization	Sample	Mineral assemblage	Method	δ³⁴S Sp	Cpy	Ga
Banded	Bes 1.1	Ep with disseminated sulphides	Laser		0.1	
Banded	Bes 1.4	Ep with disseminated sulphides	Laser	0.2	0.8	-1.2
Banded	Bes 1.5	Ep with disseminated sulphides	Laser	-1.5	0,7	
Banded	Bes 1.6	Massive sphalerite with minor Act-Ep	Laser	0.4		
Banded	Bes 1.7	Ep + sulphides disseminated and in veinlets	Laser	-0.1	-1.1	
Banded	Bes 1.9	Ep + sulphides disseminated and in veinlets	Laser	1.5	0.3	
Banded	Bes 1.9	Ep + sulphides disseminated and in veinlets	Laser	1.8	1.0	
Banded	Bes 1.10	Massive sphalerite with minor Act-Ep	Laser	-0.3	-0.4	-0.8
Banded	Bes 1.10	Massive sphalerite with minor Act-Ep	Laser	0.3		
Banded	Bes 1.10	Massive sphalerite with minor Act-Ep	Laser			12.3
Banded	Bes 1.10	Massive sphalerite with minor Act-Ep	Laser			0.9
Banded	Bes 1.11	Massive sphalerite with minor Act-Ep	Laser	-0.6		
Banded	Bes 1.12	Massive sphalerite with minor Act-Ep	Laser	0.2		
Banded	Bes 1.12	Massive sphalerite with minor Act-Ep	Laser	-0.4	0.8	0.7
Banded	Bes 2.5.3	Ep-Qz with disseminated sulphides	Laser	1.3		
Banded	Bes 2.r.3	Ep-Qz with disseminated sulphides	Laser	0.3	2.1	
Banded	Bes 1.c.1	Ep-Qz with disseminated sulphides	Laser		0.6	0.0
Banded	Bes 1.c.2	Ep-Qz with disseminated sulphides	Laser			0.3
Banded	BS 1.4a	Ep-Qz with disseminated sulphides	c.f.	-0.3		
Banded	BS1. 4b	Ep-Qz with disseminated sulphides	c.f.	-0.3		
Banded	BS1.4c	Ep-Qz with disseminated sulphides	c.f.	0		-0.6
Banded	BS1.4d	Ep-Qz with disseminated sulphides	c.f.		2.1	
Banded	BS1. 4e	Ep-Qz with disseminated sulphides	c.f.		1.8	
Irregular	Bes 3.1	Qz-Grs-Chl-Dol with disseminated sulphides	Laser	6.8		-0.1
Irregular	Bes.3.2	Qz-Grs-Chl-Dol with disseminated sulphides	Laser	4.7		7.8
Irregular	Bes 3.3	Qz-Grs-Chl-Dol with disseminated sulphides	Laser	0.4		1.1
Irregular	Bes 3.5-1	Qz-Grs-Chl-Dol with disseminated sulphides	Laser	20.5	19.8	
Irregular	Bes 3.5-2	Qz-Grs-Chl-Dol with disseminated sulphides	Laser	7.9		
Irregular	Bes 3.5-3	Qz-Grs-Chl-Dol with disseminated sulphides	Laser	11.1		
Irregular	Bes 3.5-4	Qz-Grs-Chl-Dol with disseminated sulphides	c.f.			0.8
Breccia	Bes 3.6		Laser	0.8	-1.1	0.4
Banded	Bs 6a	Ep-Qz with disseminated sulphides	c.f.	1.1		-0.2
Banded	Bs 6b	Ep-Qz with disseminated sulphides	c.f.	1.2	1.5	-0.2
Banded	Bs 6c	Ep-Qz with disseminated sulphides	c.f.			0.2
Banded	Bs 6d	Ep-Qz with disseminated sulphides	c.f.		2	
Banded	Bs 2a	Ep-Qz with disseminated sulphides	c.f.	0.2	1.6	0.2
Banded	Bs 6e	Ep-Qz with disseminated sulphides	c.f.			1.1

c.f., continuous flow isotope ratio mass spectrometry; Act, actinolite-tremolite; Chl, chlorite; Cpy, chalcopyrite; Dol, dolomite; Ep, epidote; Gn, galena; Grs, grossular; Qz, quartz, Sp, sphalerite.

TABLE 4 | Oxygen and carbon isotope data of carbonates

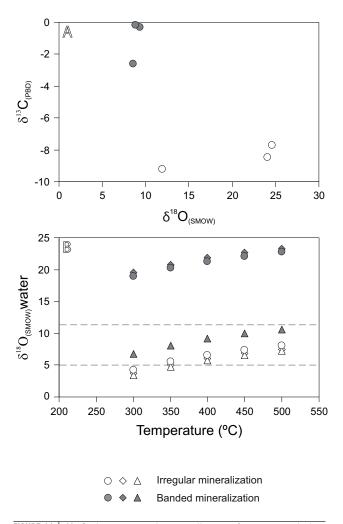| Sample	Mineral	δ¹³C V-PDB (‰)	δ¹⁸O V-PDB (‰)	δ¹⁸O V-SMOW (‰)
Bes 2.4.1	Calcite in Calcsilicate layers	-0.1	-21.43	8.8
Bes 2.4.1	Calcite in Calcsilicate layers	-2.6	-21.66	8.5
Bes 2.R.2	Recrystallized dolomicrite	-0.3	-20.90	9.3
Bes 3.2	Calcite vein	-7.7	-6.09	24.6
Bes 3.5	Limestone with galena and chlorite	-9.2	-18.42	11.9
Bes 3.2	Recrystallized dolomicrite	-8.5	-6.62	24.0

FIGURE 11 A) Carbon–oxygen isotope diagram for measured data from carbonate minerals of banded and irregular mineralisations. B) Calculated oxygen isotope compositions of hydrothermal fluids based on the equation of O'Neal *et al.* (1969). Dashed lines indicate the field of magmatic oxygen.

5) The relatively wide range in the salinity values of fluid inclusions could be explained by a) a boiling process, or b) as a result of the mixing of two different fluids, one with low salinity and the other with high salinity. There is no evidence of boiling, thus a possible process of mixing must be taken into account. The existence of a wide range of salinities in fluid inclusions has been reported in many skarn deposits, which are attributed to a mixing process of two fluids at the time of mineral formation (Blackwell and Zaw, 2001; Niiranen *et al.*, 2005). In addition, some fluid inclusions from both the banded and irregular mineralisation indicate the presence of a low salinity fluid, with about 1.2wt% NaCl eq. This salinity is lower than most of those reported in SEDEX deposits (Gardner and Hutchinson, 1985; Samson and Russell, 1987; Ansdell *et al.*, 1989), although low salinity fluids have been reported in modern vents in the Guaymas Basin, Gulf of California

(Peter *et al.*, 1986). An interaction with meteoric fluids, as suggested for the retrograde stage at many skarn deposits (Haynes and Kesler, 1988; Logan, 2000), could also produce low salinity fluid inclusions.

6) $\delta^{13}C$ in the host dolomicrites and in calcite associated to the ores shows a variation from -9.2 to -0.1‰. These values are in accordance with a marine origin of carbonates. Nevertheless, the calculated $\delta^{18}O$ values of water in equilibrium with carbonates from the banded mineralisation (between 300° and 500°C) overlap the range of the magmatic fluids, whereas those values from the irregular mineralisation are higher than the expected magmatic values. Thus, carbon in the hydrothermal calcite has its origin in the dissolution of the host dolomicrites, whereas oxygen results from the interaction with a fluid of magmatic origin.

The mineral assemblages and textures, as well as fluid inclusion and isotope data, are in agreement with a process of interaction between magmatic fluids and the sedimentary host rocks. These fluids were sulphur-rich and produced an extensive sulphide banded mineralisation. A second input of fluids interacted with the previous mineralisation giving way to a new irregular mineralisation with a broader range in the composition of the minerals. In addition, the new fluid was sulphide-rich and its interaction with the previous sulphides gave way to a wide range of the $\delta^{34}S$ values. The origin of the last fluids could be late magmatic, contemporary with the formation of the magmatic breccia, as is typical of the late stages of magmatic crystallisation. However, a meteoric component of the fluid cannot be completely ruled out.

The absence of a large intrusive body near the deposit indicates a distal position of the deposit with respect to the main igneous source. Most Zn-rich skarns occur distally with respect to associated igneous rocks (Meinert *et al.*, 2005; Canet *et al.*, 2009). The relatively low homogenization temperatures of fluid inclusions support this proposal.

CONCLUSIONS

The Pb-Zn-Cu deposit of Ulldemolins is hosted by lower Namurian turbiditic sequences consisting of interbedded sandstones, pelites, conglomerates and shales. The mineral assemblage of the deposit consists of sulphide-bearing calc-silicates, epidote, Ca-amphiboles and Ca-garnet. This mineral assemblage is characteristic of retrograde stage of skarns. The dominant textures suggest that the whole deposit was formed by a complex, multi-event, replacive process that developed selectively along a dolomicrite bed. Such process produced two different

styles of mineralisation: i) irregular, massive skarn, and ii) banded skarn.

Isotopic analyses of carbonates ($\delta^{13}C$ and $\delta^{18}O$) and sulphides ($\delta^{34}S$) from the banded mineralisation present a narrow range of values ($\delta^{13}C$ from -2.6‰ to -0.1‰, $\delta^{18}O$ from 8.5‰ to 9.3‰ and ^{34}S from -1.5 to +2.1‰) located within the range of magmatic values. Nevertheless, the irregular mineralisalition has a wide range ($\delta^{13}C$ from -9.2‰ to -7.7‰, $\delta^{18}O$, from 6.9‰ to 12.5‰ and $\delta^{34}S$ from -1.5 to +20.5‰). These data are consistent with an ore mineralisation formed by the interaction of magmatic hydrothermal fluids with carbonate host rocks.

Micrometric measurements of fluid inclusions indicate that the ore fluid has a wide salinity range suggesting that two fluids were involved in the formation of the deposit: i) early magmatic fluids separated from the melt by exsolution, and ii) fluids that ascend through fractures formed during the granite porphyry emplacement. The latter two could be late magmatic fluids that were modified by interaction with the host metasedimentary rocks and with meteoric water.

ACKNOWLEDGMENTS

REFERENCES

Alfonso, P., Canet, C., Melgarejo, J.C., Fallick, A.E., 2002. Sulphur isotope compositions of shale-hosted PGE-Ag-Au-Zn-Cu mineralisations of the Prades Mountains (Catalonia, Spain). Mineralium Deposita, 37, 198-212.

Anadón, P., Julivert, M., Sáez, A., 1985. El Carbonífero de las Cadenas Costeras Catalanas. In: Martínez, C. (ed.). X Congreso Internacional de Estratigrafía y Geología del Carbonífero y Pérmico en España. Madrid, Instituto Geológico y Minero de España (IGME), 99-106.

Ansdell, K.M., Nesbitt, B.E., Longstaffe, F.J., 1989. A fluid inclusion and stable isotope study of the Tom Ba-Pb-Zn deposit, Yukon Territory, Canada. Economic Geology, 84, 841-856.

Bakker, R.J., 2003. Package FLUIDS 1. New computer programs for the analysis of fluid inclusion data and for modelling bulk fluid properties. Chemical Geology, 194, 3-23.

Blackwell, S., Zaw, K., 2001. A petrological and fluid inclusion study of magnetite–scheelite skarn mineralisation at Kara, Northwestern Tasmania: implications for ore genesis. Chemical Geology, 173, 239-253.

Bodnar, R.J., 1993. Revised equation and table for determining the freezing point depression of H_2O–NaCl solutions. Geochimica et Cosmochimica Acta, 57, 683-684.

Canals, A., Cardellach, E., 1997. Ore lead and sulphur isotope pattern from the low-temperature veins of the Catalonian Coastal Ranges (NE Spain). Mineralium Deposita, 32, 243-249.

Canet, C., 2001. Dipòsits sedimentàrio-exhalatius del Paleozoic del SW dels Catalànides: model de dipòsit. Doctoral Thesis. Universitat de Barcelona, 442pp.

Canet, C., Alfonso, P., Melgarejo, J.C., Fallick, A.E., 2005. Stable isotope geochemistry of the carboniferous Zn-Pb-Cu sediment-hosted sulphide deposits from the southern Catalonian Coastal Ranges, Spain. International Geology Review, 47, 1298-1315.

Canet, C., Camprubí, A., González-Partida, E., Linares, C., Alfonso, P., Piñeiro-Fernández, F., Prol-Ledesma, R.M., 2009. Mineral assemblages of the Francisco I. Madero Zn-Cu-Pb-(Ag) deposit, Zacatecas, Mexico: implications for ore deposit genesis. Ore Geology Reviews, 35, 423-435.

Ciobanu, C.L., Cook, N.J., 2004, Skarn textures and a case study: the Ocna de Fier-Dognecea orefield, Banat, Romania. Ore Geology Reviews, 24, 315-370.

Einaudi, M.T., 1982. General features and origin of skarns associated with porphyry copper plutons, southwestern North America. In: Titley, S.R. (ed.). Advances in Geology of the Porphyry Copper Deposits, Southwestern U.S. United States of America (USA), University of Arizona Press, 185-209.

Enrique, P., Debon, F., 1987. Le pluton permien calcoalcalin du Montnegre (Chaînes Cotières Catalanes, Espagne); étude isotopique Rb-Sr et comparaison avec les granites hercyniens des Pyrénées, Sardaigne et Corse. Les Comptes Rendus de l'Académie des Sciences de Paris, série II, 35, 1157-1162.

Fallick, A.E., McConville, P., Boyce, A.J., Burgess, R., Kelley, S.P., 1992. Laser microprobe stable isotope measurements on geological materials. Some experimental considerations (with special reference to $\delta^{34}S$ in sulphides). Chemical Geology, 101, 53-61.

Gardner, H.D., Hutchinson, I., 1985. Geochemistry, mineralogy and geology of the Janson Pb-Zn deposits, Macmillan Pass, Yukon, Canada. Economic Geology, 80, 1257-1276.

Giesemann, A., Jäger, H.J., Norman, A.L., Krouse, H.R., Brand, W.A., 1994. On-line sulfur-isotope determination using an elemental analyzer coupled to a mass spectrometer. Analytical Chemistry. 66, 2816-2819.

Hall, A.J., McConville, P., Boyce, A.J., Fallick, A.E., 1994. Sulphides with high $\delta^{34}S$ from the Late Precambrian Bonahaven Dolomite, Argyll, Scotland. Mineralogical Magazine, 58, 486-490.

Haynes, F.M, Kesler, S.E., 1988. Compositions and sources of mineralizing fluid for chimney and manto limestone-replacement ores in Mexico. Economic Geology, 83, 1985-1992.

Leake, B.E., Woolley, A.R., Arps, C.E.S., Birch, W.D., Gilbert, M.C., Grice, J.D., Hawthorne, F.C., Kato, A., Kisch, H.J., Krivovichev, V.G., Linthout, K., Laird, J., Mandarino, J., Maresch, W.V., Nickel, E.H., Schumacher, J.C., Smith, D.C., Stephenson, N.C.N., Ungaretti, L., Whittaker, E.J.W., Youzhi, G., 1997. Nomenclature of amphiboles: Report of the subcommittee on amphiboles of the International Mineralogical Association Commission on new minerals and mineral names. Canadian Mineralogist, 35, 219-246.

Logan, A.M.V., 2000. Mineralogy and geochemistry of the Gualilán skarn deposit in the Precordillera of western Argentina. Ore Geology Reviews, 17, 113-138.

McCrea, J.M., 1950. On the isotopic chemistry of carbonates and a paleotemperature scale. Journal of Chemical Physics, 18, 849-857.

Meinert, L.D., 1993. Igneous petrogenesis and skarn deposits. Geological Association of Canada, 40 (Special Paper), 569-583.

Meinert, L.D., Dipple, G.M., Nicolescu, S., 2005. World skarn deposits. Economic Geology, 100th Anniversary Volume, 299-336.

Melgarejo, J.C., 1992. Estudio geológico y metalogenético del Paleozoico del sur de las Cordilleras Costero Catalanas. Memorias del Instituto Tecnológico Geominero de España, 103, 605pp.

Melgarejo, J.C., Ayora, C., 1984. Mineralización filoniana de tungsteno en rocas graníticas del sector S de las Cordilleras Costero Catalanas. Boletín Geológico y Minero de España, 95, 235-245.

Niiranen, T., Mänttäri, I., Poutiainen, M., Oliver, N.H.S., Millar, J.A., 2005. Genesis of Palaeoproterozoic iron skarns in the Misi region, northern Finland. Mineralium Deposita, 40, 192-217.

Ohmoto, H., Rye, R.O., 1979. Isotopes of sulfur and carbon. In: Barnes, H.L. (ed.). Geochemistry of Hydrothermal Ore Deposits. New York, Willey and Sons, 2nd edition, 509-567.

O'Neil, J.R., Clayton, R.N., Mayeda, T.K., 1969. Oxygen isotope fractionation in divalent metal carbonates. Journal of Chemical Physics, 51, 5547-5558.

Peter, J.M., Scott, S.D., Shanks, W.C.III, Woodruff, L.G., 1986. Geochemical, mineralogical, fluid inclusion and stable isotope studies of hydrothermal vent precipitates, Guaymas Basin, Gulf of California. In: Turner, R.J.W., Einaudi, M.T., (eds.). The genesis of stratiform sediment-hosted lead and zinc deposits. Conference Proceedings. Stanford University Publications in the Geological Sciences, 20, 151-155.

Roedder, E., 1984. Fluid Inclusions. In: Ribbe, P.H. (ed.). Reviews in mineralogy, 12. Mineralogical Society of America, Reviews in Mineralogy, 12, 644pp.

Sáez, A., 1982. Estudio estratigráfico y sedimentológico de los materiales paleozoicos de la parte central del Priorat (Tarragona). PhD. Thesis. Universitat de Barcelona, 86pp.

Samson, I.M., Russell, M.J., 1987. Genesis of the Silvermines zinc-lead-barite deposit, Ireland: fluid inclusion and stable isotope evidence. Economic Geology, 82, 371-394.

Sanz-López, J., Melgarejo, J.C., Crimes, Th.J., 2000. Stratigraphy of Lower Cambrian and unconformable Lower Carboniferous beds from the Valls Unit (Catalonian Coastal Ranges). Les Comptes Rendus de l'Académie des Sciences de Paris, série IIa, Sciences de la Terre, 330, 147-153.

Vilaseca, S., 1973. Reus y su entorno en la prehistoria, volume I-II. Reus (Spain), Asociación de Estudios Reusenses, 286pp.